ELSEVIER

Analytica Chimica Acta 385 (1999) 223–240

ANALYTICA CHIMICA ACTA

Scanning electrochemical microscopy: beyond the solid/liquid interface

Anna L. Barker, Marylou Gonsalves, Julie V. Macpherson, Christopher J. Slevin, Patrick R. Unwin*

Department of Chemistry, University of Warwick, Coventry CV4 7 AL, UK

Received 23 July 1998; accepted 11 August 1998

Abstract

Recent progress has seen scanning electrochemical microscopy (SECM) emerge as a powerful technique for probing physicochemical interfacial processes, beyond the solid/liquid and electrode/electrolyte interfaces that were originally of primary interest. This review (with 92 references) assesses recent developments in SECM as a methodology for investigating liquid/liquid and liquid/gas interfaces, along with processes of biochemical and biophysical significance.

Keywords: Ultramicroelectrodes; Liquid/liquid interface; Liquid/gas interface; Kinetics; Permeability

1. Introduction

It is 10 years since the term ''scanning electrochemical microscopy'' (SECM) was introduced by Bard et al. [1] to describe an instrument in which a mobile ultramicroelectrode (UME), in an electrolyte solution, was scanned in close proximity to a solid surface to characterise the topography and redox activity of the solid/liquid interface. The formulation of a theory for SECM [2] and further applications [3] provided a framework for a diversity of subsequent developments in this field. SECM itself has its origins in earlier in situ electrochemical scanning tunnelling microscopy (STM) studies from Bard's group [4] and simultaneous work by Engstrom et al. [5,6], who were the first to show that an amperometric UME could be used as a local probe to map the concentration profile of a larger active electrode. The field has now matured to a status where, at the time of writing, there are more than 280 published papers [7] and commercial instruments are available [8,9].

The original primary interest in SECM was as a tool for characterising and probing electrode/electrolyte interfaces, e.g. (i) mapping topography [3]; (ii) for modification purposes [10] and (iii) in the investigation of electrochemical dynamics. The latter topic encompasses reactivity imaging of electrodes [11], heterogeneous electron transfer kinetics [12–14], redox processes at semiconductors [15,16], coupled solution reaction kinetics [17], and processes in polymer modified electrodes [18,19]. SECM studies of

*Corresponding author. Fax: +44-1203-524112; e-mail: p.r.unwin@warwick.ac.uk

0003-2670/99/$ – see front matter
PII: S0003-2670(98)00588-1

electrochemical phenomena continue to be important, as illustrated by recent investigations of corrosion [20–22]. It has also been demonstrated that SECM can provide unique quantitative insights into reactions at solid/liquid interfaces which lie outside the traditional boundaries of electrochemistry. This aspect of SECM is exemplified by investigations of adsorption/desorption phenomena [23]and dissolution processes [24] involving electrically insulating solids.

The diversity of interfaces and processes that can be studied with SECM continues to further increase, and now includes liquid/liquid and liquid/gas interfaces, and materials of biological significance. The aim of this review is to focus on these latest developments and to identify future promising areas for the application of SECM. The emphasis is on the most recent work, with particular consideration of investigations from our group and related studies elsewhere. Earlier applications of SECM have been reviewed extensively [25–29].

2. Principles, techniques and instrumentation

2.1. Probes

SECM (Figs. 1 and 2) employs a mobile UME tip, operated under potentiostatic or potentiometric control, to probe the properties of a target interface. The type of electrode used depends on the particular process under investigation. Amperometry, in which a target species is consumed or generated at the probe UME, can be used to induce and monitor a specific interfacial process, or simply to detect a particular species involved in an interfacial process (vide infra). Typically, amperometry involves electrolysis at a solid electrode, but the polarised interface between two immiscible electrolyte solutions (ITIES) can be used to drive electrolysis processes [30]. This type of probe can also be used to amperometrically detect ions which cannot be determined by conventional electrolysis at solid electrodes, e.g. K^+ [31].

In terms of solid electrodes, the most popular are disc-shaped, with diameters of 0.6–25 μm, formed by sealing a wire of the material of interest, usually Pt, C or Au, in a glass capillary, making an electrical connection and polishing the end flat [1,3,25,32,33]. For most SECM studies, the ratio of the diameter of the entire tip end (electrode plus surrounding insulator, $2r_s$) to that of the electrode itself, $2a$, $RG=r_s/a$ is typically around 10. Metal electrodes down to the nanometre scale can also be fabricated by sealing an etched Pt or Pt–Ir wire in a suitable insulating material, leaving just the etched end exposed [34,35]. If the SECM measurement involves simple non-invasive detection, then potentiometry, as well as amperometry, becomes a possibility, greatly extending the range of species and processes that can be investigated [36].

2.2. Positioning

The tip is attached to positioners, which allow it to be moved and positioned relative to the sample interface. A variety of positioners have been employed in SECM instruments, with the choice depending on the type of measurement and spatial resolution required. For the highest (nanometre) resolution, piezoelectric positioners similar to those used in STM are mandatory [4]. Piezoelectric ''inchworm'' motors developed by Burleigh (Fishers, NJ) have been the most popular choice for SECM instruments, offering high resolution positioning capabilities with long range travel [1,3]. A photograph of a typical SECM device, built in our laboratory, based on this type of positioner (with integrated optical encoders), is shown in Fig. 2. There has also been some use of stepper motors to control the position of the tip in the x–y plane [37–39], parallel to the interface of interest, which have proved to be particularly successful when the positions of the translational stages can be monitored independently with encoder devices. As discussed later in this paper, many SECM measurements simply involve the translation of a tip towards and/or away from a specific spot on an interface, in the perpendicular (z) direction. In this situation, it is only necessary to have high resolution z-control of the tip, typically using a piezoelectric positioner, while manual stages suffice for the other two axes [24,40]. Indeed, it has further been shown that SECM measurements can be made with manual stages on all axes, with the z-axis driven by a differential micrometer and the x–y stages controlled by fine adjustment screws. This simple cost-effective set-up allows tip approach measurements (discussed in Section 2.4) to be made with a spatial resolution of ca. ±0.25 μm [41,42].

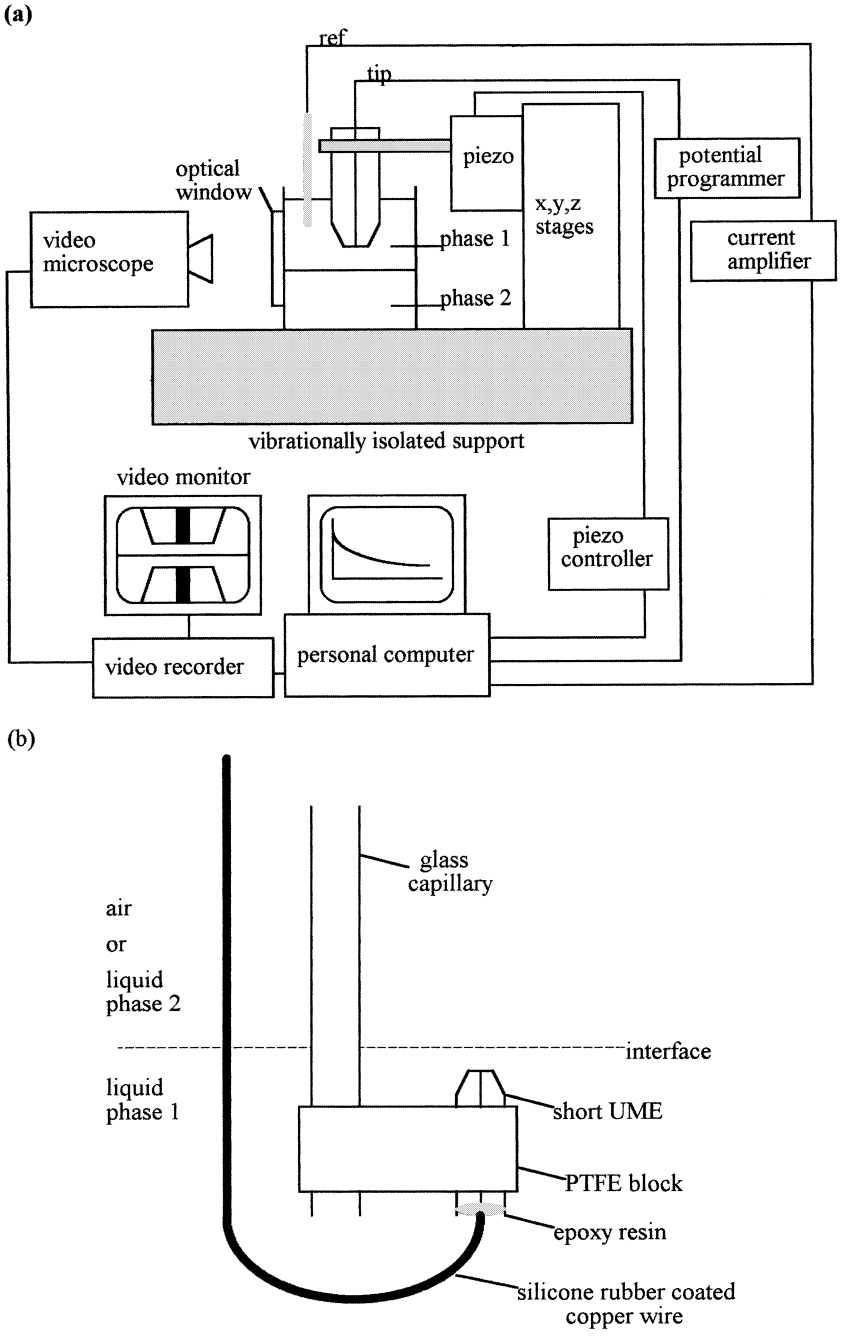

Fig. 1. (a) Block schematic of the typical instrumentation for SECM with an amperometric UME tip. The tip position may be controlled with various micropositioners, as outlined in the text (piezoelectric elements in the schematic). The tip potential is controlled with a potential programmer with respect to a reference electrode, and the current is measured with a simple amplifier device. The tip position may be viewed using a video microscope. (b) Schematic of the submarine UME configuration, to facilitate interfacial electrochemical measurements when the phase containing the UME is more dense than the second phase. In this case, the glass capillary is attached to suitable micropositioners and electrical contact is made via the insulated copper wire shown.

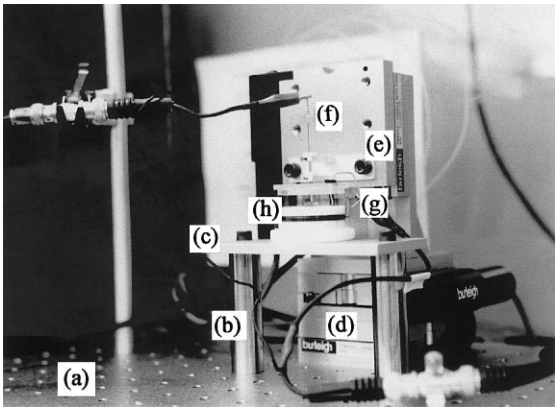

Fig. 2. Photograph of the stages and cell for a typical SECM experiment. (a) Vibrationally isolated breadboard; (b) stainless steel cell mounting poles; (c) aluminium plate; (d) closed loop translational stages; (e) aluminium UME holder; (f) UME; (g) Ag quasi-reference electrode and (h) fully detachable cell.

2.3. Electrochemical instrumentation

The electrochemical circuitry required for SECM is relatively straightforward. For amperometric control of the tip, with externally unbiased interfaces, as in many of the studies described in this paper, a simple two-electrode system suffices (Fig. 1). A potential is applied to the tip, with respect to a suitable reference electrode, to drive the process of interest and the corresponding current which flows is typically amplified by a current to voltage converter. Potentiometric detection with UMEs of various types is readily accomplished [36,43], typically using a voltage follower with an input impedance appropriate to the type of indicator electrode used.

2.4. Modes of operation

One of the attractive features of SECM is that the tip response, with all the electrode types highlighted above, is based on well-established electrochemical principles, making the technique quantitative. This aspect of SECM is well illustrated by considering the case of simple diffusion-limited electrolysis at an amperometric disc-shaped tip. When the tip is positioned a long way from the target interface, $d>10a$, where d is the tip/interface, it behaves as a conventional UME. In this situation, a steady-state current, $i(\infty)$, is rapidly established due to hemispherical diffusion of the target species (Ox in Fig. 3(a)). As the tip is brought close to an interface which is inert with respect to the species involved in the electrode process, diffusion to the UME becomes hindered (Fig. 3(b)) and the steady-state current, i, decreases compared to $i(\infty)$. In general, measurements of $i/i(\infty)$ as a function of d are termed ''approach curves''.

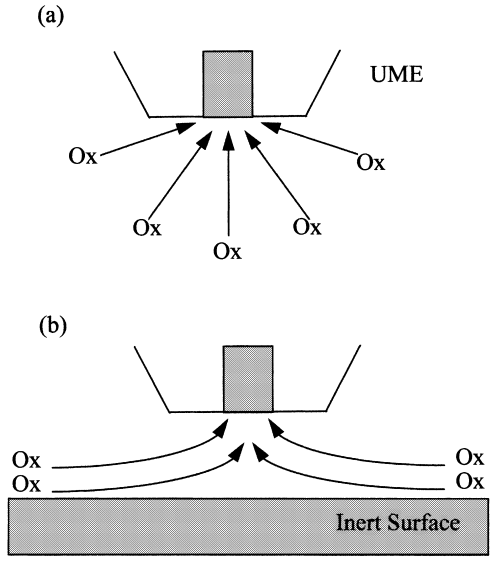

Fig. 3. (a) Schematic of the hemispherical diffusion-field established for the steady-state diffusion-limited reduction of Ox at a disc-shaped UME placed in a solution. (b) When the UME is positioned close to an inert target interface, diffusion of Ox is hindered and the current, i, is less than that measured in (a), defined as $i(\infty)$.

Since the dependence of the $i/i(\infty)$ ratio on d and the tip geometry can be calculated theoretically [2], simple current measurements of this type can also be used to provide information on the topography of a sample. In this application, an amperometric UME is typically scanned in a constant x–y plane above the target interface and the diffusion-limited current for the electrolysis of the target species measured. This, in turn, can then be related to a distance between the tip and the interface, from which topographical information is obtained.

When either the solution species of interest, or electrolysis product(s), interact with the target interface, the hindered mass transport picture of Fig. 3(b) is modified. The effect is manifested in a change in the tip current, which is the basis of using SECM to investigate interfacial reactivity. It is worth noting

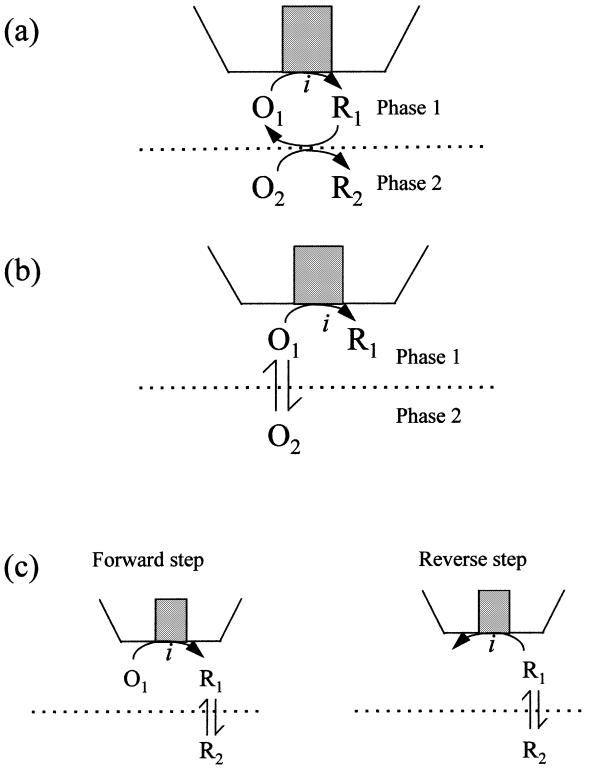

Fig. 4. Principal methods for inducing and monitoring interfacial processes with SECM: (a) feedback mode; (b) induced transfer and (c) double potential step chronoamperometry.

that, under these conditions, independent methods for determining topography of the sample are often useful. Recently developed non-electrochemical methods of imaging sample topography by detecting the shear force damping of a tip oscillated at resonant frequency appear to be particularly promising [44,45].

Hitherto, there are primarily three ways in which an amperometric electrode can be used to simultaneously induce and monitor interfacial processes. These are illustrated schematically in Fig. 4 for the most general case where diffusion may occur in both the phases which comprise the interface of interest. These basic mass transport pictures are applicable to the situation where the liquid phase containing the UME is in contact with a second phase which has fluid-like transport properties (e.g. a second immiscible liquid, polymeric material or a gas). Transport processes in phase 2 can usually be neglected when phase 2 is a solid or a gas (due to the rapidity of transport in gases compared to liquids).

The feedback mode (Fig. 4(a)) is one of the most widely used SECM techniques, applicable to the study of interfacial redox processes. The basic idea is to generate a species at the tip in its oxidised or reduced state (generation of R_1 in Fig. 4(a)), typically at a diffusion-controlled rate, by electrolysis of the other half of a redox couple (O_1). The tip-generated species diffuses from the UME to the interface. If it undergoes a redox reaction which converts it to the original form, it diffuses back to the tip, thereby establishing a feedback cycle and enhancing the current at the UME. The redox reaction may: (i) either occur at a fixed site on the interface, as in the case of immobilised oxidoreductase enzymes discussed in Section 3.2 or (ii) require the diffusion of a partner species in phase 2 to the interface (O_2 in Fig. 4(a)), as in the case of electron transfer at immiscible liquid/liquid interfaces discussed in Section 4.1.

SECM induced transfer (SECMIT, Fig. 4(b)) can be used to characterise reversible phase transfer processes at a wide variety of interfaces. The basic idea is to perturb the process, initially at equilibrium, through local electrolysis at the UME. The application of a potential to the tip, sufficient to deplete the species of interest in phase 1 (reduction of O_1 to R_1 in Fig. 4(b)), drives the transfer of the species O from phase 2 to phase 1. Collection of the species at the tip enhances the current flow compared to the situation where there is no net transfer and electroactive species reach the tip by hindered diffusion through phase 1 only. For a given tip/interface separation, the overall current response is governed by diffusion in phase 1 (and phase 2 if that phase has fluid properties) and the interfacial kinetics. The technique was originally employed in a time-dependent potential step chronoamperometric mode to probe desorption processes at solid/liquid interfaces [23], and was subsequently shown to be a powerful probe of dissolution kinetics under both steady-state and time-dependent operation [24]. As discussed in Sections 3.1, 4.3 and 5, the technique has very recently proven to be a powerful approach for probing the kinetics of solute transfer across interfaces formed between: (i) biological tissues and aqueous solutions; (ii) immiscible liquids and (iii) liquids and gases.

When there are no interfacial kinetic limitations to the transfer process, SECMIT is also an effective analytical technique for determining the permeability,

concentration and diffusive properties of a solute in a phase, without the UME having to enter or contact that phase, as discussed in Sections 3.1 and 4.3. This is obviously advantageous for situations where direct voltammetric measurements would otherwise be impractical, e.g., due to high resistivity, a limited solvent window, or where the UME would damage the structural integrity of the sample (as in the case of a biological tissue).

To expand the range of interfacial processes that can be studied with SECM, our group has recently introduced double potential step chronoamperometry (DPSC) for initiating and monitoring reactions on a local scale. When employed at UMEs, DPSC has proven to be a powerful technique for characterising the lifetimes of transient species involved in solution processes down to the microsecond timescale [46] and the diffusion coefficients of electrogenerated species, independent of knowledge of the concentration and number of electrons transferred [47]. In the SECM configuration, the follow-up chemical reaction involving the tip-generated species is effectively confined to the interface under study. The basic concept (Fig. 4(c)) is to employ the UME to generate a reactive species in an initial (forward) step for a fixed period. The potential is jumped from a value where there are no redox reactions to one where O_1 is reduced to R_1 at a diffusion-controlled rate. During this step, the tip-generated species (R_1) diffuses away from the UME and intercepts the interface. If the species interacts with the interface (e.g. by adsorption, absorption or a chemical reaction), its concentration profile is modified compared to the situation where there is no interaction and the species simply leaks out of the tip/interface gap by hindered diffusion.

Consequently, when the potential is reversed, in a final step to collect the species by electrolysis, the flux at the UME, and the corresponding current–time characteristics, depend strongly on the nature of the interaction of species R with the target interface. The application of this technique to probe absorption processes at liquid/liquid and liquid/air interfaces will be discussed in detail in Sections 4.2 and 5.

When amperometric or potentiometric electrodes are used as non-invasive probes of interfacial processes, their response depends on mass transport in the system, and interfacial kinetics. Consequently, when SECM is used only as a detector, there are broadly two classes of experiment: (i) the measurement of interfacial kinetics, which requires that the mass transport rates in the system are known and (ii) the determination of local mass transport rates, under conditions where interfacial kinetics are either rapid and non-limiting, or unimportant. Applications of such collection measurements to probe interfacial kinetics and measure local transport rates are discussed in Sections 3.1 and 4.4.

3. SECM of biological systems

Many of the principles and techniques described in the previous section have found particular application in studies of biological processes. Here we discuss two broad areas in which SECM has made a significant impact (Sections 3.1 and 3.2).

3.1. Transport pathways in membranes and permeability measurements in biological tissues

The transport of species between two solutions separated by a membrane or porous material is a general phenomenon underpinning a number of major processes in biological systems. Solute transport can be promoted in several ways: an applied electric field will lead to the migration of ions; a pressure difference will result in transport by convection and a concentration gradient will promote diffusion. There are several key questions to address when investigating permeability and transport processes in biological tissues. Is the rate of transport across the membrane uniform or spatially localised? If transport is localised, where are the active sites and can the local transport rate be measured quantitatively?

SECM is particularly suited to addressing these questions, since, under conditions where the UME is held at a potential to detect a specific solution species by diffusion-controlled electrolysis, the magnitude of the current flowing at the tip depends only on the local rate of mass transport. Fig. 5 illustrates schematically one approach for locating permeable regions in a target membrane which separates a donor and receptor compartment, across which mass transport occurs, by one of the processes identified above. By measuring the tip current as a function of position in the x–y plane as the probe is scanned over the

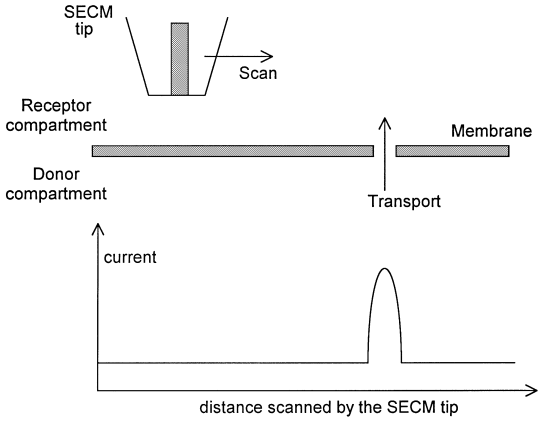

Fig. 5. Examining permeability with SECM. Transport of species by convection, diffusion or migration (promoted by pressure, concentration or electric field gradients; the latter for ions only) can be detected as an increase in the transport-limited current at a UME. A map of diffusion-limited current versus tip position can then be converted to a corresponding permeability map of the target interface.

interface of interest, active regions are identifiable from an enhancement in the current compared to the response when the tip sits above an area of the interface where transport is purely by hindered diffusion.

The first studies of this type were made by White and co-workers [48–52] who used the technique to determine the major transport pathways of solutes across track-etched polycarbonate (0.1 μm pore size) [48], punctured mica samples (pore sizes in the range 1–7 μm) [48,49], and excised hairless mouse skin [48,50,51], under the application of an electric field. These studies were aimed at providing a better understanding of the processes involved in iontophoretic drug delivery, in particular, identifying through which skin appendages transport occurred.

White's group demonstrated that, upon application of an electric field, the follicles (typical pore diameter 15–20 μm, at a density of several hundred/cm^2) in hairless mouse skin provided the dominant transport pathway, ultimately carrying almost 75% of the current (after an initial period of lower activity). Moreover, these measurements were quantitative and down to the level of a single pore. Recently, the role of the applied electric field on the transport of neutral molecules through porous membranes has been investigated [52]. With the UME positioned close to a membrane, across which an iontophoretic current was passed, SECM measurements provided quantitative information on diffusive and electro-osmotic fluxes. In particular, protocols were devised for measuring electro-osmotic drag coefficients and convective velocities of neutral electroactive molecules emerging from individual pores.

The permeability of redox mediators through voltage-gated ion channels in planar lipid membranes has also been investigated using SECM. Matsue et al. [53] measured the migration–diffusion rates of charged species such as $Fe(CN)_6^{3-}$, I^- and $Ru(NH_3)_6^{3+}$, through alamethicin ion channels. With the electrode held in a fixed position close to the membrane, ca. 400 channels were sampled, and interfacial fluxes down to 1×10^{-10} mol cm^{-2} s^{-1} were determined. The studies concluded that the channels provided a barrier to the permeation of multicharged negative ions.

Work from our group used the mass transport imaging capabilities of the SECM to quantify the rates of fluid flow through tubules in dentine slices [54–56] subjected to fluid pressures similar to in vivo pulpal pressures. Complementary studies by Nugues and Denuault [57] examined diffusive transport through dentine slices. Fluid flow through exposed dentinal tubules in the tooth is thought to be key in hypersensitivity, and it is necessary to gain a fundamental understanding of fluid movement, at a local level, to develop effective treatments. It was demonstrated, for the first time, that convective rates varied dramatically at the local level [54,55]. By using UMEs with small a (down to 1 μm), it was possible to determine the rate of convection of an electrolyte solution containing hexacyanoferrate(II) ions to the level of single tubules (2 μm diameter) [55]. Fig. 6 shows typical images of normalised transport-limited current for the oxidation of hexacyanoferrate(II) as a function of tip position in the plane parallel to the dentine surface. The data were obtained with: (a) a hydrostatic pressure of 20 cm aqueous solution across a dentine slice and (b) no solution pressure across the slice. In the latter case, the current was due to hindered diffusion of hexacyanoferrate(II), in the receptor phase containing the tip. By subtracting the data in Fig. 6(b) from those in Fig. 6(a), producing the difference plot in Fig. 6(c), regions of flow are readily visualised. For this particular case, flow was predominantly through one tubule, with several others

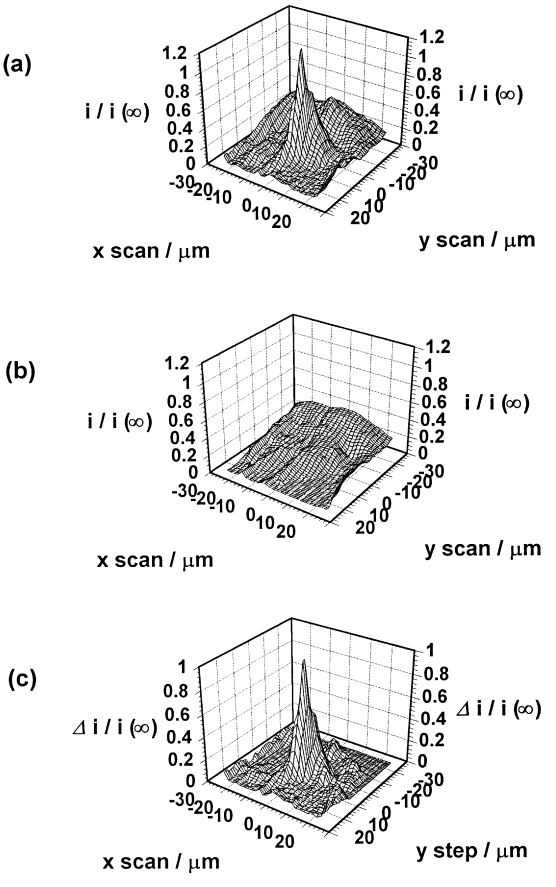

Fig. 6. Images of the variation of normalised transport-limited current for the oxidation of hexacyanoferrate(II) with a tip (a=1.0 μm) scanned in a plane parallel to a dentine surface. The data were obtained with: (a) a pressure of 20 cm aqueous solution across a 50 μm-thick dentine slice and (b) no solution pressure across the slice. The difference image (c) highlights the areas of the sample through which localised mass transport occurs.

showing limited activity. Since the 50 μm square area contained ca. 80 tubules, it was concluded that the majority of tubules in this region showed no detectable flow, probably due to occlusions sub-surface. Subsequent work investigated the effectiveness of dentinal blocking agents such as calcium oxalate [54] and glycerol mono-oleate [58] in occluding the tubules and retarding solution flow.

SECM imaging of transport in biological materials was further extended through investigations of osmotically induced convective transport of solutes through soft tissues, using $Ru(NH_3)_6^{3+}$ in pig laryngeal cartilage as a model system [59]. SECM models allowed the lateral variation of mass transport rates across the surface of cartilage to be visualised and compared directly to the corresponding topography, for the first time. Permeable areas of the tissue were identified and local fluid velocities on the μm s^{-1} scale determined. It was established that the interterritorial regions, i.e. the areas between cells in the surface of the cartilage presented to the UME, provided the most facile transport pathways.

SECMIT, discussed in Section 2.4 and shown schematically in Fig. 4(b), has significant potential for complementary mass transport measurements in biological tissues. The technique is able to probe diffusional properties accurately without the UME having to contact or enter the sample, so that the structural integrity of the tissue is maintained. SECMIT has been used successfully to measure the diffusion coefficient of oxygen in pig laryngeal cartilage. Fig. 7 shows a typical steady-state approach curve for the diffusion-limited reduction of oxygen at a 25 μm diameter Pt UME approaching a thin slice of cartilage in aerated aqueous electrolyte. Close to the interface, the measured currents are higher than predicted for an inert surface, since the electrolysis process promotes the

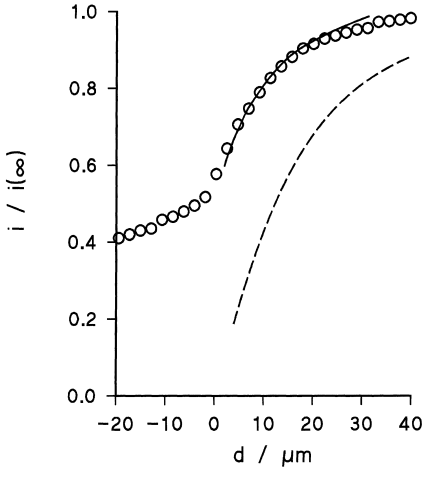

Fig. 7. Approach curve of normalised steady-state current versus probe/interface separation for the diffusion-controlled reduction of oxygen at a UME scanned towards a sample of laryngeal cartilage (○). The dashed line shows the theoretical response for an inert interface (hindered diffusion only of oxygen in the aqueous phase containing the UME), while the solid line shows the behaviour for induced transfer with the oxygen diffusion coefficient having a value 50% of that in aqueous solution. The partition coefficient for oxygen between the aqueous and cartilage phases is unity.

transfer of oxygen from the cartilage matrix to the aqueous solution, enhancing the flux at the UME. Quantitative analysis of the results indicated that the diffusion coefficient of oxygen in cartilage was ca. 50% of that in aqueous solution [59].

3.2. Redox processes on biological surfaces: photosynthesis and immobilised enzyme activity

The topography and photosynthetic electron transfer activity of stomata and single guards cells have been probed using SECM [60,61]. Bard and co-workers [60] used the SECM operating in the negative feedback mode (Fig. 3(b)) to image stomata on the surfaces of grass, *ligustrum sinensis* and elodea leaves under both dark and illuminated conditions. More recently, this group reported the detection of oxygen evolution above individual stomatal guard cells in the living leaf of the *Tradescantia flumensis* plant, as a direct consequence of photosynthetic electron transport induced by irradiation [61].

Imaging of bioelectrochemical phenomena with SECM, such as enzyme-catalysed redox reactions, can be achieved using both amperometric or potentiometric probes. In the former case, the UME may operate in either the feedback or tip collection (TC) mode. For the TC mode, and measurements with potentiometric probes, the UME is used exclusively to detect the product(s) of an enzyme-catalysed redox reaction at the target substrate. In contrast, the feedback mode employs a redox mediator in solution (together with an enzyme specific substrate), which shuttles between the tip and the target interface, establishing a feedback cycle. The two modes are thus different in their responses, in that the feedback signal always has a contribution from hindered diffusion of the mediator, as well as the interfacial kinetics, whereas the TC mode measures an absolute current due only to the product of an enzyme reaction. However, while lower enzyme activities can be detected using the TC mode, higher lateral resolution is available from the feedback mode [62].

Bard and co-workers [63] were the first to demonstrate the utility of SECM in probing immobilised enzyme kinetics, utilising the feedback mode to measure the redox activity of glucose oxidase (GO) catalysis under conditions of high D-glucose concentration. Subsequently, activity maps were obtained of: (i) GO immobilised in a membrane and (ii) mitochondrion-bound NADH-cytochrome *c* reductase [64]. Kranz et al. [65] covalently tagged microfabricated thin film structures of polypyrrole, formed on a gold substrate, with GO and used the feedback currents in the presence, and then absence, of both a redox mediator and glucose, to distinguish the enzyme sites from the underlying metallic substrate.

The micropatterning of enzymes and antigens, for use in miniaturised biosensors and immunosensors, has also been studied via the feedback mode of SECM. Matsue and co-workers [66] fabricated and characterised diaphorase-patterned surfaces at the micrometre level. Additional work by Shiku et al. [67] found that by coupling SECM with the enzyme-linked immunosorbent assay (ELISA) technique, detection levels as low as 10^4 molecules in a single 20 μm radius spot could be obtained for a carcinoembryonic antigen.

The TC mode has been used to visualise the active binding sites of immobilised antibodies [62]. In this study, the antigen binding sites were presaturated with an antigen-conjugate capable of catalytically converting a redox-inactive mediator (4-aminophenyl phosphate) to an electroactive form (4-aminophenol), which was subsequently detected at the tip UME. SECM has also been employed to image active enzyme spots on an alkanethiol-gold substrate [68]. In this application, it was necessary to use the TC mode to characterise the micropatterned structures in order to avoid unwanted feedback from uncovered gold areas, which would otherwise complicate the tip current response.

Bard and co-workers [69] have used UMEs with tips modified with polymer-entrapped horseradish peroxidase as biosensors for the detection of hydrogen peroxide produced during the enzymatic oxidation of glucose by immobilised GO. The probes had a limited pH range (ca. 4–8), and did not provide sufficient sensitivity for high resolution imaging, but they could be used to obtain concentration maps, resolved to tens of micrometres. Bard's group [43] also used potentiometric SECM probes, with urease-immobilised tips, for the detection and imaging of local enzyme activity. Using dual channel probes, with one channel as a distance sensor, they were able to overcome the difficulty of determining absolute tip position, normally encountered in potentiometric SECM experi-

ments, and imaged urease activity with high spatial resolution.

Meyer et al. [70] developed a novel technique to image glucose distribution profiles, using a microelectrode array, modified with polypyrrole-entrapped GO. In contrast to SECM methodology, where a single UME is scanned over the surface of interest, each electrode in the array was individually addressed and the electrode signals recorded successively to provide time-resolved images. Although the local resolution was ca. 500 μm, application of silicon thin-film technology should, in principle, enable a resolution of <1 μm. In addition, arrays offer the potential for multianalyte detection and the application of pattern-recognition methodology.

4. Electron, ion and molecular transfer at liquid/liquid interfaces

Measuring the kinetics of chemical processes that occur at ITIES, or – more generally – at the interface between two fluids, is currently of intense interest from both fundamental and practical perspectives. SECM has recently been shown to be a valuable technique for studying this type of system [31,71–81] overcoming several of the problems inherent in more conventional methodologies. SECM approaches employ a direct liquid/liquid contact, of well-defined area, under conditions where contributions to the overall rate from mass transport and interfacial processes can readily be resolved. Furthermore, the use of small UMEs in conjunction with close tip/interface separations results in the generation of high local mass transport rates, enabling the accurate quantitation of rapid interfacial processes.

4.1. Electron transfer kinetics using the feedback mode

Recent studies have shown that the SECM feedback mode is a powerful probe of charge transfer kinetics at ITIES, with the following advantages over more traditional approaches: (i) Voltammetric measurements can be made with highly resistive non-aqueous solvents with minimal distortion from *iR* drop and double layer charging (in transient measurements). (ii) External bias of the interface is unnecessary as the interfacial potential can readily be controlled by use of appropriate concentrations of supporting electrolyte in each phase, greatly simplifying the experimental methodology.

Several groups have used this technique to extract electron transfer kinetics at ITIES [72–77]. In this application, shown in Fig. 4(a), a UME is positioned close to the interface, in phase 1, and held at a potential sufficient to electrolyse a mediator, O_1, at a diffusion-controlled rate, generating a redox-active product R_1. This product can then diffuse to the interface where it undergoes a bimolecular redox reaction with a species O_2 in phase 2, regenerating the initial form of the mediator as shown in the following equation:

$$R_1 + O_2 \xrightarrow{k_{12}} R_2 + O_1 \quad (1)$$

where k_{12} denotes the bimolecular interfacial electron transfer rate constant. For a given tip/substrate separation, the flux of O_1 at the tip increases with k_{12}. This rate constant can be determined from the steady-state tip current response as a function of tip/interface separation. An important feature of this approach is that the feedback current signal is due exclusively to electron transfer process, allowing discrimination against the accompanying interfacial ion transfer which occurs to maintain charge neutrality.

Wei et al. [71] demonstrated that the SECM feedback mode could be used to extract the bimolecular rate constant for electron transfer between ferrocene (Fc) in phase 2 and electrogenerated $Ru(bipy)_3^{3+}$ in phase 1. The Galvani potential difference across the liquid junction was maintained constant at −71 mV. Good agreement between the measured rate constant and that predicted from Marcus theory was obtained with the assumption that the interface was 2 nm thick. For quantitative analysis of the data, it was essential that the experimental conditions were such that Fc in phase 2 was maintained at a constant composition during all measurements, thereby eliminating depletion and diffusional limitations in this phase, and simplifying the description of mass transport in the system. A numerical model has very recently been developed by our group to take account of such limitations in the second phase [78], thus extending the range of systems accessible for future study by the SECM feedback technique.

Tsionsky et al. [72] investigated the effect of potential drop across the interface on electron transfer kinetics, by varying the concentration of common supporting ions in the two phases. By measuring the apparent rate constant for the reaction between the oxidised form of zinc porphyrin in benzene and $Ru(CN)_6^{4-}$ in aqueous solution, as a function of interfacial potential, a value for the transfer coefficient $\alpha \approx 0.5$ was calculated. Based on these results, it was concluded that conventional electron transfer theories for the metal/electrolyte interface were applicable to liquid/liquid systems. Further work [73] demonstrated that interfacial electron transfer processes could be driven ''uphill''. By poising the potential difference across a 1,2-dichloroethane (DCE)/water interface, with appropriate concentrations of potential determining ions in each phase, it was shown that an electron could be transferred from a redox couple in phase 1 to a second couple in phase 2, which had a lower standard reduction potential.

A different aspect of SECM and liquid/liquid interfaces utilises an ITIES supported at the tip of a micropipette as a probe of a second interface [30]. In the first studies of this kind [30], a micropipette was filled with a concentrated electrolyte solution containing one redox couple (hexacyanoferrate(II)/(III)), while the oxidised form of a second redox couple (tetracyanoquinodimethane, TCNQ) was present at mM level in a DCE phase, in which the micropipette was immersed. By applying a potential difference between a Pt wire placed in the micropipette and a reference electrode placed in DCE, it was possible to effect the reduction of TCNQ by hexacyanoferrate(II) at the ITIES, so that the current flow was due to the diffusion of TCNQ in DCE. The practicality of the device was demonstrated by using it to image an interdigitated electrode array in the feedback mode.

4.2. Investigations of monolayers at liquid/liquid interfaces

The effect of a monolayer of adsorbed surfactant on interfacial electron transfer rates at an ITIES has been investigated, in connection with model studies of catalytic electrochemical reactions that occur between the microphases in bicontinuous microemulsions [75]. Quantitative measurements in such systems have proved to be difficult, in the past, due to uncertainties in the area of the microemulsion interface and the site of the reaction. In contrast, SECM feedback studies allowed the rate of reduction of *trans*-1,2-dibromocyclohexane by the Co(I) form of vitamin B_{12} to be measured as a function of interfacial potential drop and adsorbed surfactants.

Recent studies have demonstrated that the adsorption of saturated phospholipids at the ITIES leads to a diminution in the interfacial electron transfer rate constant [76]. However, electron transfer rate constants between redox couples with conjugated phospholipids at the interface were twice those measured with saturated phospholipids adsorbed at the interface [77]. SECM has also been used to image electron transfer rates across a mixed monolayer of conjugated and saturated phospholipids, revealing domains of relatively high and low electron transfer rates, respectively [77]. This technique may therefore be used to elucidate the structure–activity relationships in phospholipid monolayers which has implications for studies of biological membranes.

4.3. Ion and molecular transfer processes

The kinetics of ion transfer (IT) processes at liquid/liquid interfaces are considered to be rapid, and have proved to be difficult to measure with conventional approaches, that often suffer from low mass transport rates and complications from *iR* drop (and double layer charging in time-dependent modes). Building on the pioneering work of Girault and Taylor [82], who showed that such problems could be overcome if the interfacial dimensions were shrunk down to the micrometre scale, Shao and Mirkin [79] have recently introduced an ITIES supported at a nanopipette to make steady-state voltammetric measurements of very fast facilitated ion transfer across an aqueous/DCE interface. The process of interest was the transfer of K^+, facilitated by dibenzo-18-crown-6 (DB18C6), a process which had previously been considered to be diffusion-controlled. The experiment involved placing a nanopipette, filled with aqueous solution containing excess KCl, in a DCE phase containing DB18C6. The conditions were such that the tip response was limited solely by diffusion of DB18C6 in DCE and the kinetics of complexation/decomplexation in the interfacial region. Given the tiny dimensions of the tip opening (5–50 nm), steady-state

hemispherical diffusion rates were extremely high, enabling the interfacial rate constant for the complexation process to be determined as 1.3 ± 0.6 cm s^{-1} [79]. Supported ITIES of this type were later adapted for an SECM study of ion transfer processes across a second liquid/liquid interface [31].

SECMIT is particularly suitable for investigating the transfer of electroactive species (ions or neutral molecules) across liquid/liquid interfaces. To date, SECMIT has been used to investigate the kinetics of Cu^{2+} extraction and stripping between an aqueous phase (phase 1 in Fig. 4(b)) and an organic medium (DCE or heptane as phase 2) containing the oxime ligand Acorga P50 (LH) [80,81]. The extraction/stripping process, defined by the following equation, was first allowed to come to equilibrium:

$$Cu^{2+}_{(aq)} + 2LH_{(org)} \underset{\text{stripping}}{\overset{\text{extraction}}{\rightleftarrows}} CuL_{2(org)} + 2H^{+}_{(aq)} \qquad (2)$$

The interfacial transfer kinetics were then investigated by perturbing the equilibrium, through the depletion of Cu^{2+} in the aqueous phase, with a UME located in close proximity to the aqueous/organic interface. This process promoted the transfer of Cu^{2+} into the aqueous phase, via the transport and decomplexation of the cupric ion–oxime complex, resulting in an enhanced steady-state current at the UME. Approach curve measurements of the $i/i(\infty)$ ratio versus d allowed the kinetics of the transfer process to be determined unambiguously [80,81].

SECMIT has also been used as an analytical procedure to deduce the concentration and diffusion coefficient of oxygen in DCE and nitrobenzene (NB), without supporting electrolyte present [80], using the protocol outlined in Section 3.1 for the study of biological tissues. The results obtained have important implications for increasing the scope of voltammetric and amperometric analyses, because the approach adopted overcame impracticalities associated with direct voltammetric measurements in these liquids: high solution resistivity (DCE and NB) and limited cathodic solvent window (NB).

To expand the range of processes that can be studied with SECM, we have recently suggested the use of DPSC (Section 2.4, Fig. 4(c)) for the investigation of irreversible phase transfer processes [83]. This approach was used to measure the rate of transfer of Br_2 from aqueous 0.5 mol dm^{-3} sulphuric acid solution to DCE. In the forward potential step, Br_2 was generated at the tip UME through the diffusion-limited oxidation of Br^- (at mM levels). The current–time characteristics for this forward-step process provided a very accurate measure of the tip/interface separation, since the form of the transient is governed by the hindered diffusion of Br^- to the UME which, in turn, depends only on the tip–interface separation, a, and the diffusion coefficient of Br^- (and the latter two parameters are known with high precision).

The driving force for the transfer process was the enhanced solubility of Br_2 in DCE, ca. 40 times greater than that in aqueous solution. Untransferred Br_2 was recollected in the reverse step at the tip UME, by reduction to Br^-. The transfer process was found to be controlled exclusively by diffusion in the aqueous phase, but by employing short switching times, t_{switch}, down to 10 ms, it was possible to put a lower limit on the effective interfacial transfer rate constant of 0.5 cm s^{-1}. Fig. 8 shows typical forward and reverse transients from this set of experiments, presented as current (normalised with respect to the steady-state diffusion-limited current, $i(\infty)$, for the oxidation of Br^-) versus the inverse square-root of time.

4.4. Microelectrochemical measurements of spontaneous reactions

All the SECM methods highlighted so far can only be applied to interfacial process that can be induced, as well as monitored, using UMEs. To expand the range of liquid/liquid interfacial processes accessible to study, we have introduced microelectrochemical measurements at expanding droplets (MEMED) as a new experimental approach for measuring the kinetics of reactions that occur spontaneously at the interface between two immiscible liquids [84,85]. In this approach the UME is stationary and the interface is effectively translated towards the interface in a well-defined manner so that mass transport is reproducible and characterisable. Approach curves of UME response versus tip/interface separation are then used to identify the kinetics and mechanism of the interfacial process.

The interface is created by flowing a feeder liquid through a fine capillary tip at a slow rate, so that droplets form and grow periodically in a second receptor phase in a defined way, analogous to the

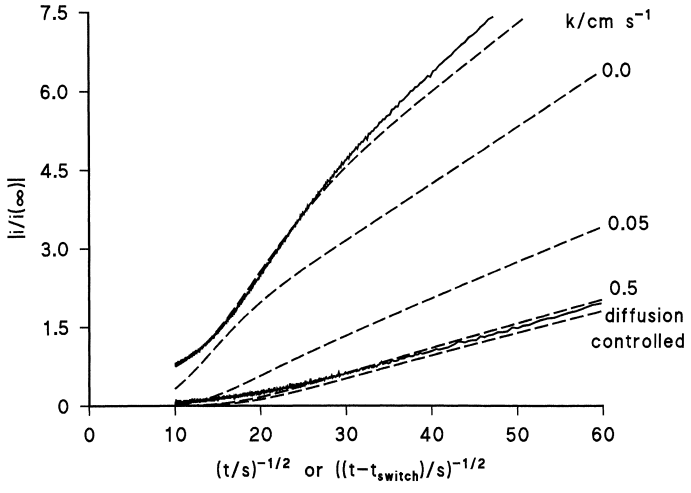

Fig. 8. Typical DPSC data (t_{switch}=10 ms) for the oxidation of 10 mM bromide (forward step; upper solid curve) and the reduction of electrogenerated Br_2 (reverse step; lower solid curve) at a 25 μm-diameter disc UME in aqueous 0.5 mol dm^{-3} sulphuric acid, at a distance of 2.8 μm from the interface with DCE. The upper dashed line is the theoretical response for the forward step at the defined tip/interface separation, with a diffusion coefficient for Br^- of 1.8×10^{-5} cm^2 s^{-1}. The remaining dashed lines are the reverse transients for irreversible transfer of Br_2 (diffusion coefficient 9.4×10^{-6} cm^2 s^{-1}) with various interfacial rate constants, k, marked on the plot.

dropping mercury electrode [86] or electrolyte dropping electrode [87]. The concentration profile of either a product or reactant extending from the droplet into the receptor phase is probed at a UME, positioned adjacent to the capillary from which the droplet expands. Both amperometric and potentiometric UMEs can be employed, facilitating the electrochemical detection of a wide range of species [85].

A schematic of the experimental apparatus with a droplet flowing down (feeder solution more dense than the receptor phase) is shown in Fig. 9. For the case where the feeder solution is less dense than the receptor phase, the capillary/detector arrangement is simply inverted. In both configurations, droplets up to 1 mm in diameter are created at a frequency of 0.05–1 s^{-1} at the tip of a glass capillary (pulled to an internal diameter of ca. 100 μm).

In initial studies [84], MEMED has been applied to investigate the hydrolysis of triphenylmethyl chloride (TPMCl) at the DCE/water interface:

$$TPMCl_{(DCE)} + H_2O \rightarrow TPMOH_{(DCE)} + H^+_{(aq)} + Cl^-_{(aq)} \quad (3)$$

The reaction rate was determined by measuring the local chloride ion concentration potentiometrically at a Ag/AgCl UME in the aqueous phase, as a droplet of DCE containing TPMCl expanded towards the electrode. A typical potentiometric transient is shown in Fig. 10, along with video microscopy images of the droplet/electrode configuration at specified times during the measurement. In the initial stages of drop growth, between (a) and (c), the electrode–drop separation is too large for chloride ions to be detected by the electrode, and background levels from the reaction of the previous drop are recorded. As the drop expands, the electrode–drop gap decreases, until at (c) the electrode intercepts the concentration boundary layer of the drop. Between (c) and (d), the chloride ion concentration in the region of the electrode increases, due to the reaction at the approaching drop surface. The contact point, (d), produces an inflexion in the transient. The shape of the concentration profile adjacent to the drop, between (c) and (d), is the key experimental measurement.

To derive kinetic information, the time-dependent concentration profile of Cl^- extending from the drop surface is extracted, using a model based on mass transport to a simple expanding sphere [84,85] together with any heterogeneous and/or homogeneous chemical reactions. Typical results for the hydrolysis of TPMCl are shown in Fig. 11. The process defined

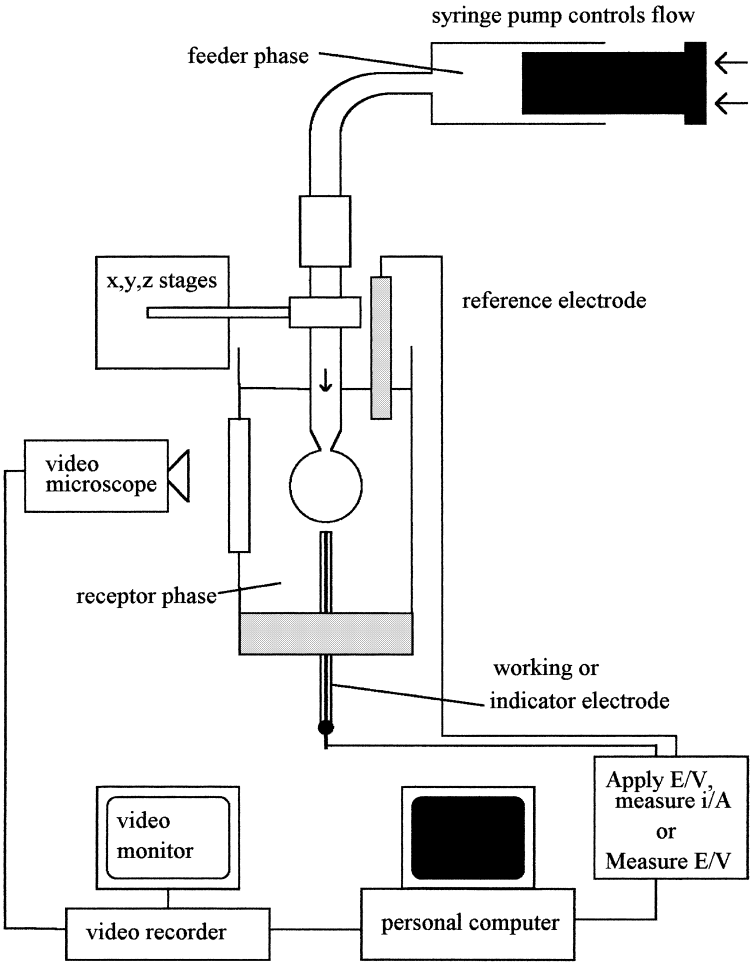

Fig. 9. Schematic (not to scale) of the experimental arrangement for MEMED with potentiometric or amperometric detection in the receptor phase. For amperometric detection, a two-electrode system is employed with the working electrode held at a value to cause the transport-limited electrolysis of the target species. With potentiometric detection, the potential between a suitable indicator electrode and a reference electrode is measured.

by Eq. (3) was found to be exclusively interfacial, and first-order in TPMCl, with a heterogeneous rate constant of 6.5×10^{-5} cm s^{-1} for the hydrolysis step.

5. Molecular transfer at the air/liquid interfaces

Our group has very recently used SECM to probe molecular transfer processes across air/water interfaces [88]. Initial work has concentrated on transfer processes with and without a monolayer of surfactant at the air/water interface. A submarine UME, as depicted schematically in Fig. 1(b), was utilised which could approach the air/water interface from below.

The first study in this area employed the DPSC mode to investigate the transfer kinetics of electrogenerated Br_2, from aqueous 0.5 mol dm^{-3} sulphuric acid to air. As found in studies of liquid/liquid interfaces [83] the rate of this irreversible transfer process (with the air phase acting as a sink) was limited only by diffusion of Br_2 in the aqueous phase. A lower limit for the interfacial transfer rate constant of 0.5 cm s^{-1} was estimated [83].

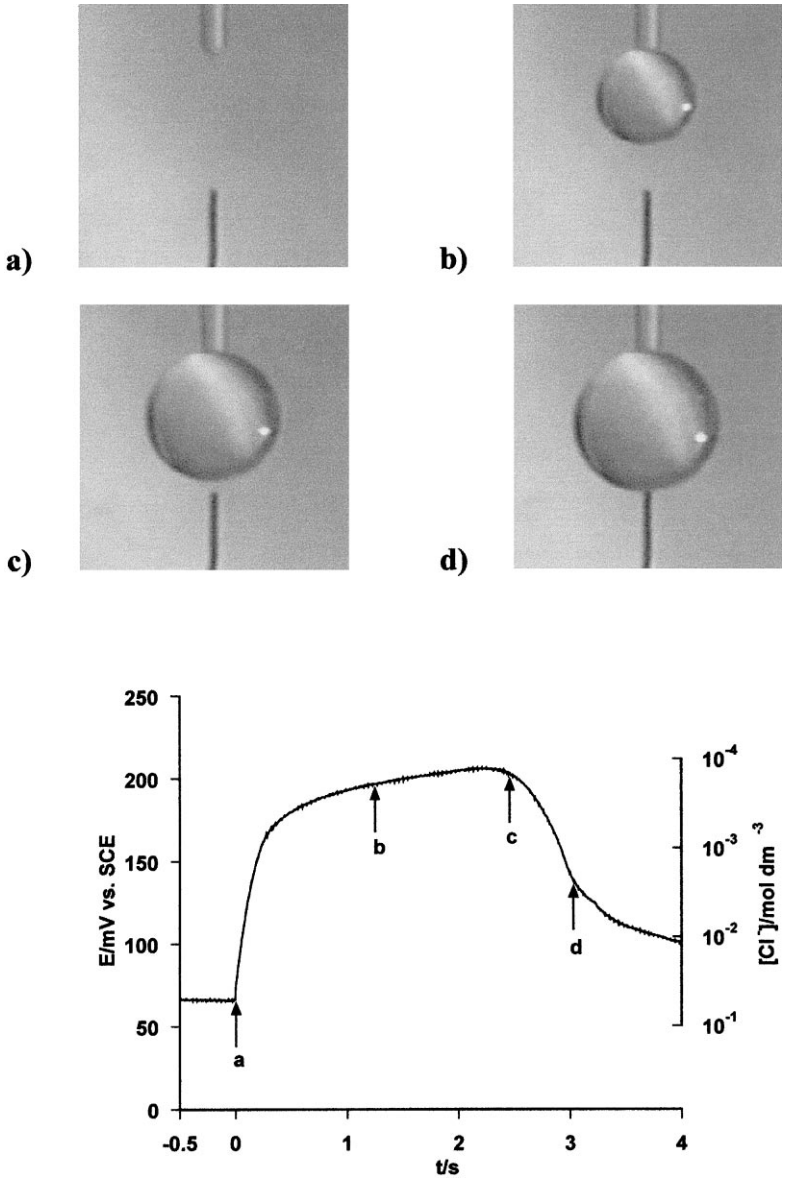

Fig. 10. Typical potentiometric transient (for Cl^-) recorded at a Ag/AgCl UME during the interfacial hydrolysis of TPMCl at a growing drop surface. The feeder solution composition was 0.100 mol dm^{-3} TPMCl in DCE, while the aqueous phase contained 0.10 mol dm^{-3} KNO_3. The time from drop birth to contact with the probe was 3.03 s. Selected video microscopy images recorded during the growth of the drop show the position of the droplet with respect to the probe at selected times during the transient. The distance separating the ends of the capillary and UME probe is 1.00 mm.

The transfer of oxygen across an air/aqueous interface in the absence and presence of a monolayer of 1-octadecanol was studied recently [88]. The interface was formed in a Langmuir trough arrangement, enabling the effect of monolayer compression on the oxygen transfer rate to be assessed. The study provided information on the effect of the monolayer on reaeration rates, which is of importance in natural

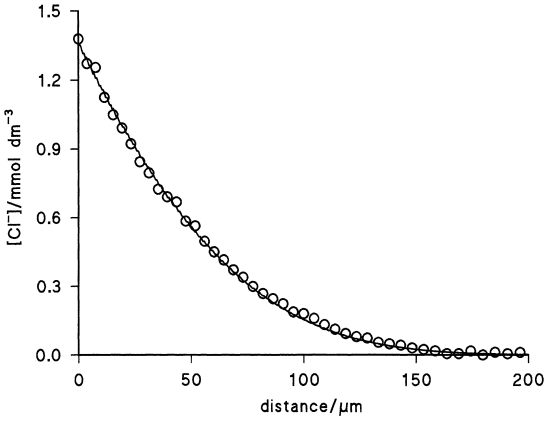

Fig. 11. Cl^- profile adjacent to an expanding drop surface recorded with a UME probe during the hydrolysis of TPMCl at the DCE/aqueous interface (○). The concentration of TPMCl in the organic phase was 0.050 mol dm^{-3}, the drop time was 4.80 s and the final drop diameter was 1.10 mm. The solid line shows the theoretical time-dependent concentration profile for interfacial hydrolysis with a first-order rate constant of 6.5×10^{-5} cm s^{-1}.

environments. The configuration could also be considered as a simple model for studies of oxygen transfer across biomembranes.

For these investigations, the UME was positioned in the aqueous subphase containing 0.1 mol dm^{-3} KNO_3 and held at a potential to reduce oxygen at a diffusion-controlled rate, in order to promote the transfer of O_2 from air (phase 2) to the aqueous solution (phase 1), with subsequent collection at the tip. Given the high diffusion coefficient and effective concentration of oxygen in the air phase, depletion effects in phase 2 were unimportant. The results of the study demonstrated that the rate of oxygen transfer across a clean air/water interface was diffusion-controlled on the timescale of SECM measurements. The rate of this transfer process was, however, significantly reduced with increasing compression of a 1-octadecanol monolayer. Fig. 12 illustrates this point, showing approach curves for oxygen reduction recorded with the monolayer at different surface pressures, along with the pressure–area isotherm for this system. The transfer rate was found to be intimately linked to the accessible free area of the interfaces, with oxygen transfer almost completely retarded in the presence of a fully compressed monolayer.

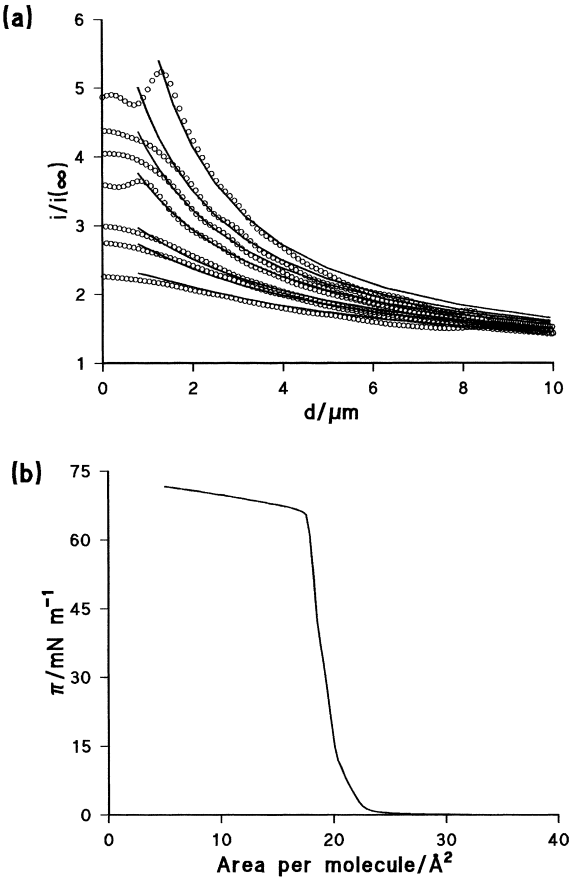

Fig. 12. (a) Normalised steady-state diffusion-limited current versus UME–interface separation for the reduction of oxygen at a UME approaching an air/water interface with 1-octadecanol monolayer coverage (○). From top to bottom, the curves correspond to an uncompressed monolayer and surface pressures of 5, 10, 20, 30, 40 and 50 mN m^{-1}. The solid lines represent the theoretical behaviour for reversible transfer in an aerated atmosphere, with zero-order rate constants for oxygen transfer from air to water/10^{-8} mol cm^{-2} s^{-1} of 6.7, 3.7, 3.3, 2.5, 1.8, 1.7 and 1.3.

6. Conclusions

The purpose of this paper has been to highlight the recent rapid progress in SECM as a probe of novel interfaces, beyond the electrode/electrolyte and solid/liquid interfaces that were initially of primary interest. This is proving to be a particularly powerful technique for investigating biological interfaces, with applications as diverse as transport in tissues through to immobilised enzyme kinetics. There is considerable

scope for additional studies in these areas, but the increased use of SECM to investigate viable (living) systems will be particularly exciting. The ability to map concentration gradients around single cells, e.g., would complement and extend the pioneering work of Wightman and others [89–92] who have already shown the utility of static UMEs for this purpose.

In a short period of time, SECM has had a significant impact on the electrochemical investigation of processes at liquid/liquid interfaces, from fundamental studies of electron and ion transfer through to industrially related processes, such as solvent extraction and hydrolysis. A myriad of processes in the biological and physical sciences involve an understanding of dynamics at fluid/fluid interfaces. It is anticipated that SECM, and related techniques, will find considerable application in tackling such processes.

The recent demonstration that SECM can be used to study liquid/gas interfaces, in general, and monolayers at air/water interfaces, opens up a number of exciting possibilities for further studies. In addition to investigations of solute transfer across organised molecular assemblies, the diverse range of SECM modes available should enable local, non-invasive studies of other types of physicochemical processes in ultrathin films, such as adsorption/desorption, lateral charge transfer and diffusion.

Acknowledgements

The support of various aspects of our SECM programme by the EPSRC, the Wellcome Trust, the Royal Society Paul Instrument Fund, Zeneca and Unilever is gratefully acknowledged. We wish to thank a number of colleagues for their contributions to some of the work described. In particular, studies of mass transport in biological systems have been carried out in conjunction with Dr. Nigel Hughes and David Littlewood (Unilever Research Port Sunlight Laboratory) and Dr. Peter Winlove (Imperial College) and Dr. Danny O'Hare (Brighton University). We have worked closely with Dr. John Atherton and John Umbers (Zeneca Huddersfield Works) on the study of liquid/liquid interfaces. Prof. David Walton and Dr. Steve Riley helped with investigations of Langmuir monolayers at air/water interfaces.

References

[1] A.J. Bard, F.-R.F. Fan, J. Kwak, O. Lev, Anal. Chem. 61 (1989) 132.
[2] J. Kwak, A.J. Bard, Anal. Chem. 61 (1989) 1221.
[3] J. Kwak, A.J. Bard, Anal. Chem. 61 (1989) 1794.
[4] H.Y. Liu, F.-R.F. Fan, C.W. Lin, A.J. Bard, J. Am. Chem. Soc. 108 (1986) 3838.
[5] R.C. Engstrom, M. Webber, D.J. Wunder, R. Burgess, S. Winquist, Anal. Chem. 58 (1986) 844.
[6] R.C. Engstrom, T. Meaney, R. Tople, R.M. Wightman, Anal. Chem. 59 (1987) 2005.
[7] http://www.msstate.edu/Dept/Chemistry/dow1/secm/secm_-bib.html, for a comprehensive list.
[8] CH Instruments Inc. 676 Germantown Parkway Suite 517, Cordova, TN 38018, USA.
[9] Quesant Scanned Probe Microscopes, Windsor Scientific Ltd., Slough, SL1 4LP, UK.
[10] A.J. Bard, G. Denuault, C. Lee, D. Mandler, D.O. Wipf, Acc. Chem. Res. 23 (1990) 357.
[11] D.O. Wipf, A.J. Bard, J. Electrochem. Soc. 138 (1991) L4.
[12] D.O. Wipf, A.J. Bard, J. Electrochem. Soc. 138 (1991) 469.
[13] A.J. Bard, M.V. Mirkin, P.R. Unwin, D.O. Wipf, J. Phys. Chem. 96 (1992) 1861.
[14] M.V. Mirkin, T.C. Richards, A.J. Bard, J. Phys. Chem. 97 (1993) 7672.
[15] B.R. Horrocks, M.V. Mirkin, A.J. Bard, J. Phys. Chem. 98 (1994) 9106.
[16] D. Mandler, A.J. Bard, J. Electrochem. Soc. 137 (1990) 2468.
[17] P.R. Unwin, A.J. Bard, J. Phys. Chem. 95 (1991) 7814.
[18] J. Kwak, C. Lee, A.J. Bard, J. Electrochem. Soc. 137 (1990) 1481.
[19] C. Lee, A.J. Bard, Anal. Chem. 62 (1990) 1906.
[20] J.W. Still, D.O. Wipf, J. Electrochem. Soc. 144 (1997) 2657.
[21] Y. Zhu, D.E. Williams, J. Electrochem. Soc. 144 (1997) L43.
[22] L.F. Garfias-Mesias, M. Alodon, P.I. James, W.H. Smyrl, J. Electrochem. Soc. 145 (1998) 2005.
[23] P.R. Unwin, A.J. Bard, J. Phys. Chem. 96 (1992) 5035.
[24] J.V. Macpherson, P.R. Unwin, J. Phys. Chem. 98 (1994) 1704; J.V. Macpherson, P.R. Unwin, J. Phys. Chem. 99 (1995) 14 824; J.V. Macpherson, P.R. Unwin, A.C. Hillier, A.J. Bard, J. Am. Chem. Soc. 118 (1996) 6445.
[25] A.J. Bard, F.-R.F. Fan, M.V. Mirkin, in: A.J. Bard (Ed.), Electroanalytical Chemistry, vol. 18, Marcel Dekker, New York, 1989.
[26] A.J. Bard, F.-R.F. Fan, D.T. Pierce, P.R. Unwin, D.O. Wipf, F. Zhou, Science 254 (1991) 68.
[27] M. Arca, A.J. Bard, B.R. Horrocks, T.C. Richards, D.A. Treichel, Analyst 119 (1994) 719.
[28] P.R. Unwin, J.V. Macpherson, Chem. Ind. 21 (1995) 874.
[29] M.V. Mirkin, Anal. Chem. 68 (1996) 177A.
[30] T. Solomon, A.J. Bard, Anal. Chem. 67 (1995) 2787.
[31] Y. Shao, M.V. Mirkin, J. Electroanal. Chem. 439 (1997) 137.
[32] R.M. Wightman, D.O. Wipf, in: A.J. Bard (Ed.), Electroanalytical Chemistry, vol. 15, Marcel Dekker, New York, 1989, p. 267.
[33] C. Lee, C.J. Miller, A.J. Bard, Anal. Chem. 63 (1991) 78.

[34] A.A. Gerwirth, D.H. Craston, A.J. Bard, J. Electroanal. Chem. 261 (1989) 477.
[35] R.M. Penner, M.J. Heben, T.L. Longin, N.S. Lewis, Science 250 (1990) 1118.
[36] D. Amman, Ion-Selective Microelectrodes, Springer, Berlin, 1986.
[37] C. Kranz, M. Ludwig, H.E. Gaub, W. Schuhmann, Adv. Mater. 7 (1995) 38.
[38] C. Kranz, M. Ludwig, H.E. Gaub, W. Schuhmann, Adv. Mater. 7 (1995) 568.
[39] P. Hliva, I. Kapui, L. Czako, G. Nagy, Magyar Kemiai Folyoirat 104 (1998) 223.
[40] J.V. Macpherson, P.R. Unwin, J. Chem. Soc., Faraday Trans. 89 (1993) 1883.
[41] R.D. Martin, P.R. Unwin, Anal. Chem. 70 (1998) 276.
[42] R.D. Martin, P.R. Unwin, J. Electroanal. Chem. 439 (1997) 123.
[43] C. Wei, A.J. Bard, G. Nagy, K. Toth, Anal. Chem. 67 (1995) 1346.
[44] M. Ludwig, C. Kranz, W. Schuhmann, H.E. Gaub, Rev. Sci. Instrum. 66 (1995) 3857.
[45] P.I. James, L.F. Garfias-Mesias, P.J. Moyer, W.H. Smyrl, J. Electrochem. Soc. 145 (1998) L64.
[46] C.P. Andrieux, P. Hapiot, J.M. Savéant, J. Phys. Chem. 92 (1988) 5992.
[47] J.V. Macpherson, P.R. Unwin, Anal. Chem. 69 (1997) 2063.
[48] E.R. Scott, H.S. White, J.B. Phipps, Anal. Chem. 65 (1993) 1537.
[49] E.R. Scott, H.S. White, J.B. Phipps, J. Membr. Sci. 58 (1991) 71.
[50] E.R. Scott, A.I. Laplaza, H.S. White, J.B. Phipps, Pharm. Res. 10 (1993) 1699.
[51] E.R. Scott, J.B. Phipps, H.S. White, J. Invest. Dermatol. 104 (1995) 142.
[52] B.D. Bath, R.D. Lee, H.S. White, E.R. Scott, Anal. Chem. 70 (1998) 1047.
[53] T. Matsue, H. Shiku, H. Yamada, I. Uchida, J. Phys. Chem. 98 (1994) 11001.
[54] J.V. Macpherson, M.A. Beeston, P.R. Unwin, N.P. Hughes, D.L. Littlewood, Langmuir 11 (1995) 3959.
[55] J.V. Macpherson, M.A. Beeston, P.R. Unwin, N.P. Hughes, D. Littlewood, J. Chem. Soc., Faraday Trans. 91 (1995) 1407.
[56] P.R. Unwin, J.V. Macpherson, M.A. Beeston, N.J. Evans, N.P. Hughes, D. Littlewood, Adv. Dent. Res. 11 (1997) 548.
[57] S. Nugues, G. Denuault, J. Electroanal. Chem. 408 (1996) 125.
[58] J.V. Macpherson, P.R. Unwin, N.P. Hughes, D. Littlewood, in preparation.
[59] J.V. Macpherson, D. O'Hare, P.R. Unwin, C.P. Winlove, Biophys. J. 73 (1997) 2771.
[60] C. Lee, J. Kwak, A.J. Bard, Proc. Natl. Acad. Sci. 87 (1990) 1740.
[61] M. Tsionsky, Z.G. Cardon, A.J. Bard, R.B. Jackson, Plant Physiol. 113 (1997) 895.
[62] G. Wittstock, K.-J. Yu, B. Halsall, T.H. Ridgeway, W.R. Heineman, Anal. Chem. 67 (1995) 3578.
[63] D.T. Pierce, P.R. Unwin, A.J. Bard, Anal. Chem. 64 (1992) 1795.
[64] D.T. Pierce, A.J. Bard, Anal. Chem. 65 (1993) 3598.
[65] C. Kranz, G. Wittstock, H. Wohlschläger, W. Schuhmann, Electrochim. Acta 42 (1997) 3105.
[66] H. Shiku, T. Takeda, H. Yamada, T. Matsue, I. Uchida, Anal. Chem. 67 (1995) 312.
[67] H. Shiku, T. Matsue, I. Uchida, Anal. Chem. 68 (1996) 1276.
[68] G. Wittstock, W. Schuhmann, Anal. Chem. 69 (1997) 5059.
[69] B.R. Horrocks, D. Schmidtke, A. Heller, A.J. Bard, Anal. Chem. 65 (1993) 3605.
[70] H. Meyer, H. Drewer, B. Gründig, K. Cammann, R. Kakerow, Y. Manoli, W. Mokwa, M. Rospert, Anal. Chem. 67 (1995) 1164.
[71] C. Wei, A.J. Bard, M.V. Mirkin, J. Phys. Chem. 99 (1995) 16033.
[72] M. Tsionsky, A.J. Bard, M.V. Mirkin, J. Phys. Chem. 100 (1996) 17881.
[73] T. Solomon, A.J. Bard, J. Phys. Chem. 99 (1995) 17487.
[74] Y. Selzer, D. Mandler, J. Electroanal. Chem. 409 (1996) 15.
[75] Y. Shao, M.V. Mirkin, J.F. Rusling, J. Phys. Chem. B 101 (1997) 3202.
[76] M. Tsionsky, A.J. Bard, M.V. Mirkin, J. Am. Chem. Soc. 119 (1997) 10785.
[77] M.-H. Delville, M. Tsionsky, A.J. Bard, Langmuir 14 (1998) 2774.
[78] A.L. Barker, P.R. Unwin, in preparation.
[79] Y. Shao, M.V. Mirkin, J. Am. Chem. Soc. 119 (1997) 8103.
[80] A.L. Barker, J.V. Macpherson, C.J. Slevin, P.R. Unwin, J. Phys. Chem. B 102 (1998) 1586.
[81] C.J. Slevin, J.A. Umbers, J.H. Atherton, P.R. Unwin, J. Chem. Soc., Faraday Trans. 92 (1996) 5177.
[82] G. Taylor, H.H.J. Girault, J. Electroanal. Chem. 208 (1986) 179.
[83] C.J. Slevin, J.V. Macpherson, P.R. Unwin, J. Phys. Chem. B 101 (1997) 10851.
[84] C.J. Slevin, P.R. Unwin, Langmuir 13 (1997) 4799.
[85] C.J. Slevin, P.R. Unwin, in preparation.
[86] C.M.A. Brett, A.M. Oliveira Brett, Electrochemistry, Oxford University Press, Oxford, 1993, p. 158.
[87] S. Kihara, M. Suzuki, K. Ogura, S. Umetani, M. Matsui, Z. Yoshida, Anal. Chem. 58 (1986) 2954.
[88] C.J. Slevin, S. Ryley, D.J. Walton, P.R. Unwin, Langmuir, 14 (1998) 5331.
[89] E.R. Travis, R.M. Wightman, Annu. Rev. Biophys. Biomol. Struct. 27 (1998) 77 and references therein.
[90] Q. Xin, R.M. Wightman, Anal. Chem. 70 (1998) 1677 and references therein.
[91] P.S. Cahill, Q.D. Walker, J.M. Finnegan, G.E. Mickelson, E.R. Travis, R.M. Wightman, Anal. Chem. 68 (1996) 3180 and references therein.
[92] R.M. Wightman, Interface 5 (1996) 22.